iScience

CellPress
OPEN ACCESS

Article

TOPK mediates immune evasion of renal cell carcinoma via upregulating the expression of PD-L1

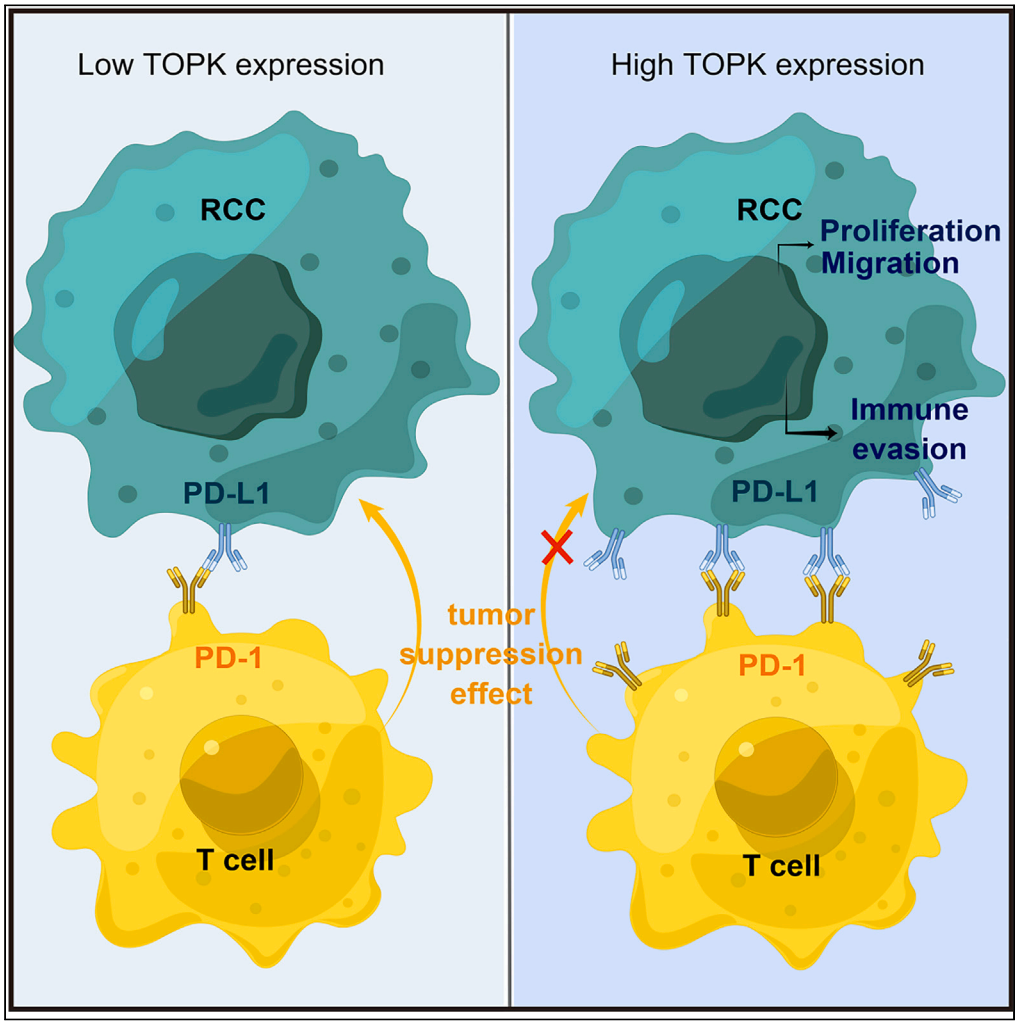

Jinxin Li, Huimin Sun, Meiling Fu, ..., Yue Zhao, Zhiyuan Shi, Chen Shao

cshao@xah.xmu.edu.cn

Highlights

High expression of TOPK in renal cell carcinoma predicts poor prognosis

Activation of TOPK promotes PD-L1-mediated immune escape in renal cell carcinoma

The presence of TOPK is required for the TGF-β/Smad pathway to function

TOPK inhibition offers new ideas for renal cell carcinoma treatment

Li et al., iScience 26, 107185
July 21, 2023
https://doi.org/10.1016/j.isci.2023.107185

iScience

CellPress
OPEN ACCESS

Article

TOPK mediates immune evasion of renal cell carcinoma via upregulating the expression of PD-L1

Jinxin Li,[1,3] Huimin Sun,[1,2,3] Meiling Fu,[1] Zeyuan Zheng,[1] Chunlan Xu,[1] Kunao Yang,[1] Yankuo Liu,[1] Zuodong Xuan,[1] Yang Bai,[1] Jianzhong Zheng,[1] Yue Zhao,[1] Zhiyuan Shi,[1] and Chen Shao[1,4,*]

SUMMARY

Although anti-PD-L1 therapy has been used in the clinical treatment of renal cell carcinoma (RCC), a proportion of patients are not sensitive to it, which may be attributed to the heterogeneity of PD-L1 expression. Here, we demonstrated that high TOPK (T-LAK cell-originated Protein Kinase) expression in RCC promoted PD-L1 expression by activating ERK2 and TGF-β/Smad pathways. TOPK was positively correlated with PD-L1 expression levels in RCC. Meanwhile, TOPK significantly inhibited the infiltration and function of $CD8^+$ T cells and promoted the immune escape of RCC. Moreover, inhibition of TOPK significantly enhanced $CD8^+$ T cell infiltration, promoted $CD8^+$ T cell activation, enhanced anti-PD-L1 therapeutic efficacy, and synergistically enhanced anti-RCC immune response. In conclusion, this study proposes a new PD-L1 regulatory mechanism that is expected to improve the effectiveness of immunotherapy for RCC.

INTRODUCTION

Renal cell carcinoma (RCC), originating from renal tubular epithelial cells or renal cortex, is one of the most common malignant tumors of the urinary system, accounting for about 80–90% of malignant renal tumors.[1] The most frequent histotype is clear cell carcinoma (ccRCC), which accounts for 70–80% of RCC cases.[2,3] Given that RCC is not sensitive to radiotherapy[4] and chemotherapy,[5] surgical resection remains the mainstay of treatment for early localized RCC.[6] However, it should be borne in mind that even after partial or radical nephrectomy, RCC can progress to advanced or metastatic disease, which requires more comprehensive therapies.[7] For more than a decade, the first choice of treatment for advanced RCC has been targeted therapy, mainly based on drugs directed against the VEGF/VEGFR pathway.

With the widespread application of immunotherapy in clinical tumors in recent years, anti-PD-1/PD-L1-based immune checkpoint inhibitors (ICIs) have been used to treat various malignant tumors, including RCC.[8] The effectiveness of ICIs in combination with targeted therapies has been demonstrated and is recommended for the treatment of metastatic RCC(mRCC).[9–11] However, there are still some RCC patients with poor sensitivity to ICI treatment, which may be related to the expression level of PD-L1.[12,13] PD-L1 expression is regulated by multiple mechanisms and can even be altered by prior therapies.[13] Therefore, exploring effective and stable PD-L1 regulatory mechanisms and molecular targets is necessary to improve anti-PD-L1 therapeutic efficacy.

TOPK is lymphokine-activated killer T cell-derived protein kinase, also known as PDZ-binding kinase(PBK), highly expressed in a variety of malignant tumor cells and is closely related to the occurrence and development of tumors.[14–16] As a member of the mitogen-activated protein kinase kinase (MAPKK) family, TOPK mostly acts through the MAPK pathway and is mainly involved in cell dynamics, cell cycle regulation, DNA damage and repair.[17] Few studies have been hitherto reported on the relationship between TOPK and RCC. Our previous study showed that the phosphorylation of TOPK S32 significantly promotes tumorigenesis and is involved in sorafenib resistance in RCC, which suggests that TOPK may play an important role in RCC.[18] Meanwhile, Dong-Hee Lee et al. found that TOPK could influence the level of immune cell infiltration in colon cancer.[19] Moreover, Tingting Feng et al. found that TOPK was associated with T cell function infiltrating in RCC by bioinformatics, suggesting that TOPK may affect immune evasion in RCC, although the exact mechanism is unknown.[20]

In this study, we substantiated that TOPK could promote PD-L1 expression and inhibit T cell function, promoting immune escape in RCC. Moreover, inhibition of TOPK significantly enhanced sensitivity to

[1]Department of Urology, Xiang'an Hospital of Xiamen University, School of Medicine, Xiamen University, Xiamen 361101, China

[2]Central Laboratory, Xiang'an Hospital of Xiamen University, School of Medicine, Xiamen University, Xiamen 361101, China

[3]These authors contributed equally

[4]Lead contact

*Correspondence: cshao@xah.xmu.edu.cn

https://doi.org/10.1016/j.isci.2023.107185

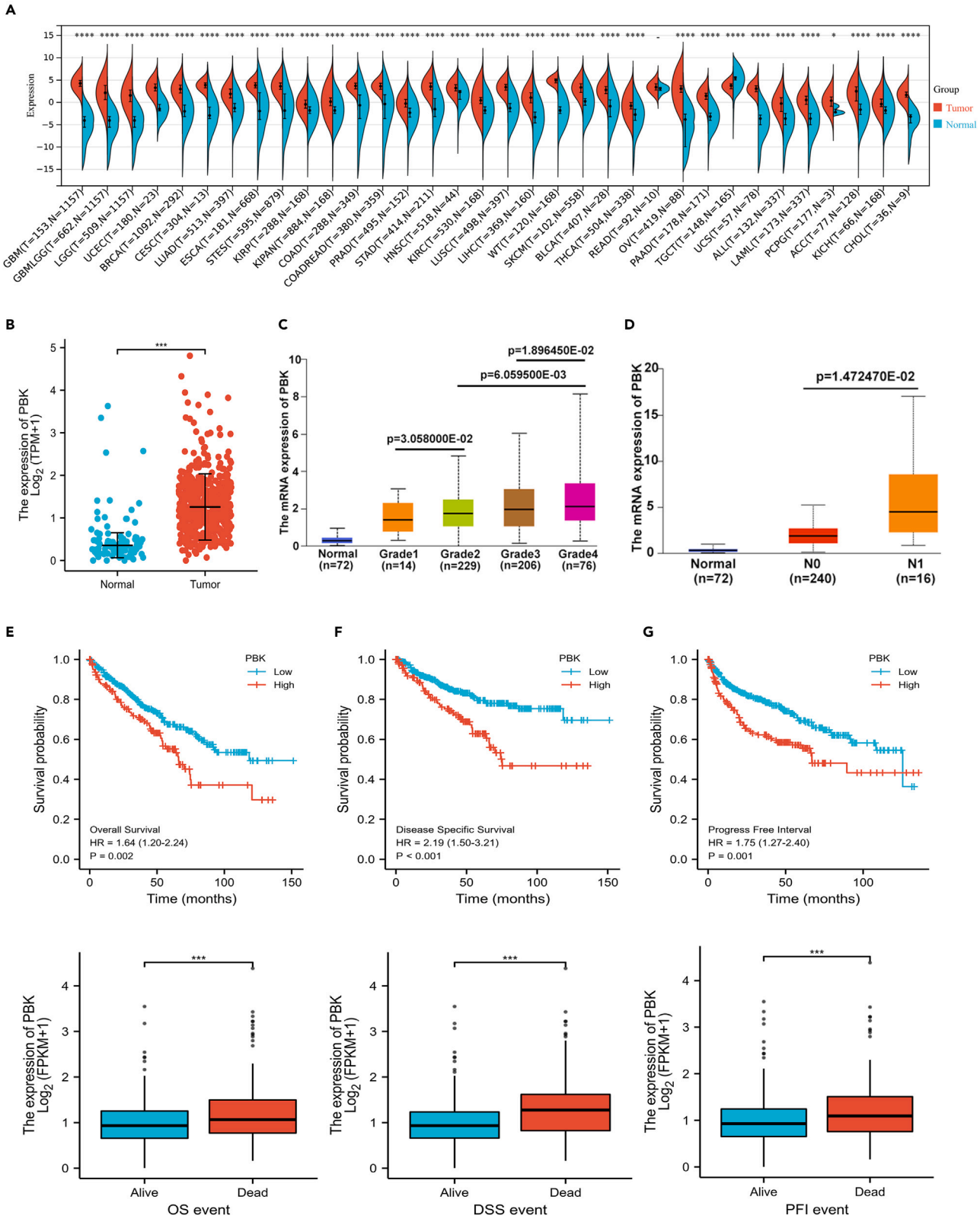
A
Expression
Group
Tumor
Normal
GBM(T=153,N=1157)
GBMLGG(T=662,N=1157)
LGG(T=509,N=1157)
UCEC(T=180,N=23)
BRCA(T=1092,N=292)
CESC(T=304,N=13)
LUAD(T=513,N=397)
ESCA(T=181,N=668)
STES(T=595,N=879)
KIRP(T=288,N=168)
KIPAN(T=884,N=168)
COAD(T=288,N=349)
COADREAD(T=380,N=359)
PRAD(T=495,N=152)
STAD(T=414,N=211)
HNSC(T=518,N=44)
KIRC(T=530,N=168)
LUSC(T=498,N=397)
LIHC(T=369,N=160)
WT(T=120,N=168)
SKCM(T=102,N=558)
BLCA(T=407,N=28)
THCA(T=504,N=338)
READ(T=92,N=10)
OV(T=419,N=88)
PAAD(T=178,N=171)
TGCT(T=148,N=165)
UCS(T=57,N=78)
ALL(T=132,N=337)
LAML(T=173,N=337)
PCPG(T=177,N=3)
ACC(T=77,N=128)
KICH(T=66,N=168)
CHOL(T=36,N=9)
B
The expression of PBK
Log2 (TPM+1)
Normal
Tumor
C
The mRNA expression of PBK
p=3.058000E-02
p=6.059500E-03
p=1.896450E-02
Normal (n=72)
Grade1 (n=14)
Grade2 (n=229)
Grade3 (n=206)
Grade4 (n=76)
D
The mRNA expression of PBK
p=1.472470E-02
Normal (n=72)
N0 (n=240)
N1 (n=16)
E
Survival probability
PBK
Low
High
Overall Survival
HR = 1.64 (1.20-2.24)
P = 0.002
Time (months)
F
Survival probability
PBK
Low
High
Disease Specific Survival
HR = 2.19 (1.50-3.21)
P < 0.001
Time (months)
G
Survival probability
PBK
Low
High
Progress Free Interval
HR = 1.75 (1.27-2.40)
P = 0.001
Time (months)
The expression of PBK
Log2 (FPKM+1)
Alive
Dead
OS event
DSS event
PFI event

Figure 1. TOPK is highly expressed and is associated with poor prognosis in patients with RCC

The expression and prognosis of TOPK in RCC from the TCGA database was analyzed.

(A) TOPK expression in pan-cancer.

(B) TOPK expression in RCC as well as in para-cancerous tissue.

(C) Relationship between TOPK and different stage grading of RCC.

(D) Relationship between TOPK and RCC lymph node metastasis status.

(E–G) Relationship between TOPK and different survival stages of RCC. OS (Overall Survival), DSS (Disease-Specific Survival), and PFI (Progression-Free Interval) were analyzed. Data are expressed as mean ± SD. *p < 0.05, **p < 0.01, ***p < 0.001, ns, not significant.

anti-PD-L1 therapy, providing meaningful insights into kidney cancer treatment. Overall, TOPK is a valuable molecular marker that can be applied in the prognostic prediction of kidney cancer patients and as a potential therapeutic target.

RESULTS

TOPK is highly expressed in RCC and correlates with a poor prognosis in patients with renal cancer

We first analyzed the expression of TOPK in cancer using The Cancer Genome Atlas (TCGA) database(https://portal.gdc.cancer.gov/). The results showed that TOPK expression in various tumors was significantly higher than in the corresponding normal tissues (Figure 1A). Further analysis revealed that TOPK was significantly higher expressed in RCC (Figure 1B). Also, its expression closely correlated with tumor grade, with higher levels of TOPK expression in higher tumor grades (Figure 1C). RCC with lymph node metastasis expressed higher levels of TOPK compared to tumors without lymph node metastasis (Figure 1D). At the same time, the high expression of TOPK in RCC patients was correlated with a low survival rate in terms of overall survival (OS), disease-specific survival (DSS), or progression-free interval (PFI) (Figures 1E–1G). These results suggest that TOPK may be a poor prognostic factor in RCC and that high TOPK expression may predict advanced clinical staging and poor prognosis in this patient population.

TOPK enhances the proliferation and migration of RCC cells

Subsequently, we examined TOPK expression in several renal cancer cell lines. As shown in the figure (Figure 2A), TOPK exhibited high expression in ACHN and 786-O cells but low expression in Caki-1 and SN12C cells. Accordingly, 786-O and Caki-1 were selected for experiments (Figures 2B and 2C). To further verify the effect of TOPK on RCC, we performed cell proliferation and migration experiments using TOPK knockdown and overexpressing cell lines, respectively. The MTT and EDU proliferation assay revealed that TOPK overexpression significantly promoted the proliferation of RCC cells, whereas knockdown yielded the opposite findings (Figures 2D–2G). Next, we verified the cell migration ability by transwell cell migration (Figures 2H and 2I) and wound healing assays (Figures S1A–S1B). The results showed that TOPK overexpression significantly enhanced the migratory ability of RCC cells, whereas knockdown yielded the opposite findings. The above results indicated that TOPK significantly affects RCC cells by promoting their growth and metastatic abilities.

TOPK inhibits the function of cytotoxic $CD8^+$ T cells infiltrating in RCC tissues

Although TOPK can improve the proliferation and migration ability and promote the progression of RCC, it remains unclear whether it can affect the immune system in RCC. Data from TCGA database(https://portal.gdc.cancer.gov/) was used to analyze whether TOPK correlated with immune cell infiltration in RCC and we found that TOPK significantly correlated with the infiltration level of immune cells. In this respect, we found increased infiltration levels of T cells, macrophages and Treg cells and decreased infiltration of NK cells (Figure 3A). This finding suggests that TOPK may be an immunosuppressive factor. To further explore the effect of TOPK on the immunity of RCC, we knocked down TOPK by stable transfection in Renca, a mouse renal cancer cell line with high TOPK expression (Figure 3B). Next, we used the control and TOPK-KD Renca cells to induce subcutaneous tumors on the back of BALB/C mice, respectively. The tumor formation and detection protocols are shown in the figure (Figure 3C). Importantly, we found that the subcutaneous tumor volume and weight were significantly reduced in mice injected with TOPK-KD cells compared with controls (Figures 3D–3F). At the same time, compared with the control group, the percentage of subcutaneous tumor-infiltrating $CD8^+$ T cells in mice injected with TOPK-KD cells was significantly increased (Figure 3G). CD107a and CD69 are important markers of T cell activation, expressing on the surface of activated $CD8^+$ T cells.[21] We found that compared with the control group, the percentage of $CD8^+$ T cells expressing CD107a and CD69 was also significantly increased (Figure 3H). In addition, a preliminary

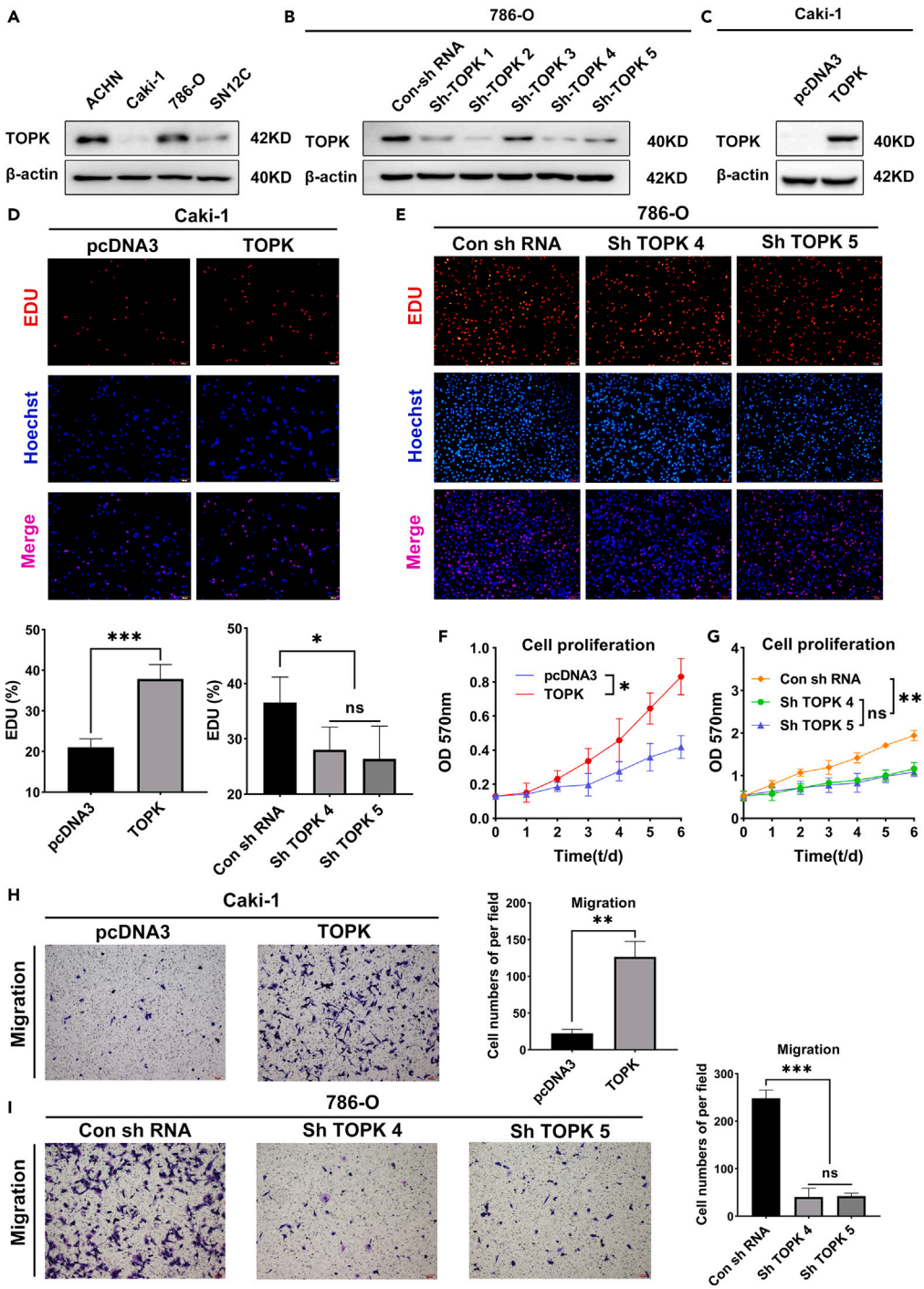

Figure 2. TOPK enhances the proliferation and migration of RCC cells

(A) TOPK expression was examined in different kidney cancer cell lines.

(B–C) TOPK knockdown and overexpression cell lines were established using 786-O and Caki-1 cells, respectively.

(D–E) Representative images of 786-O and Caki-1 cell EDU assays and EDU+ cell percentages were analyzed.

(F–G) Cell proliferation of 786-O and Caki-1 cells was detected with MTT assays.

(H–I) Representative images and statistical analysis results of transwell migration experiments for 786-O and Caki-1 cells, respectively. Data are expressed as mean ± SD. *p < 0.05, **p < 0.01, ***p < 0.001, ns, not significant. See also Figure S1.

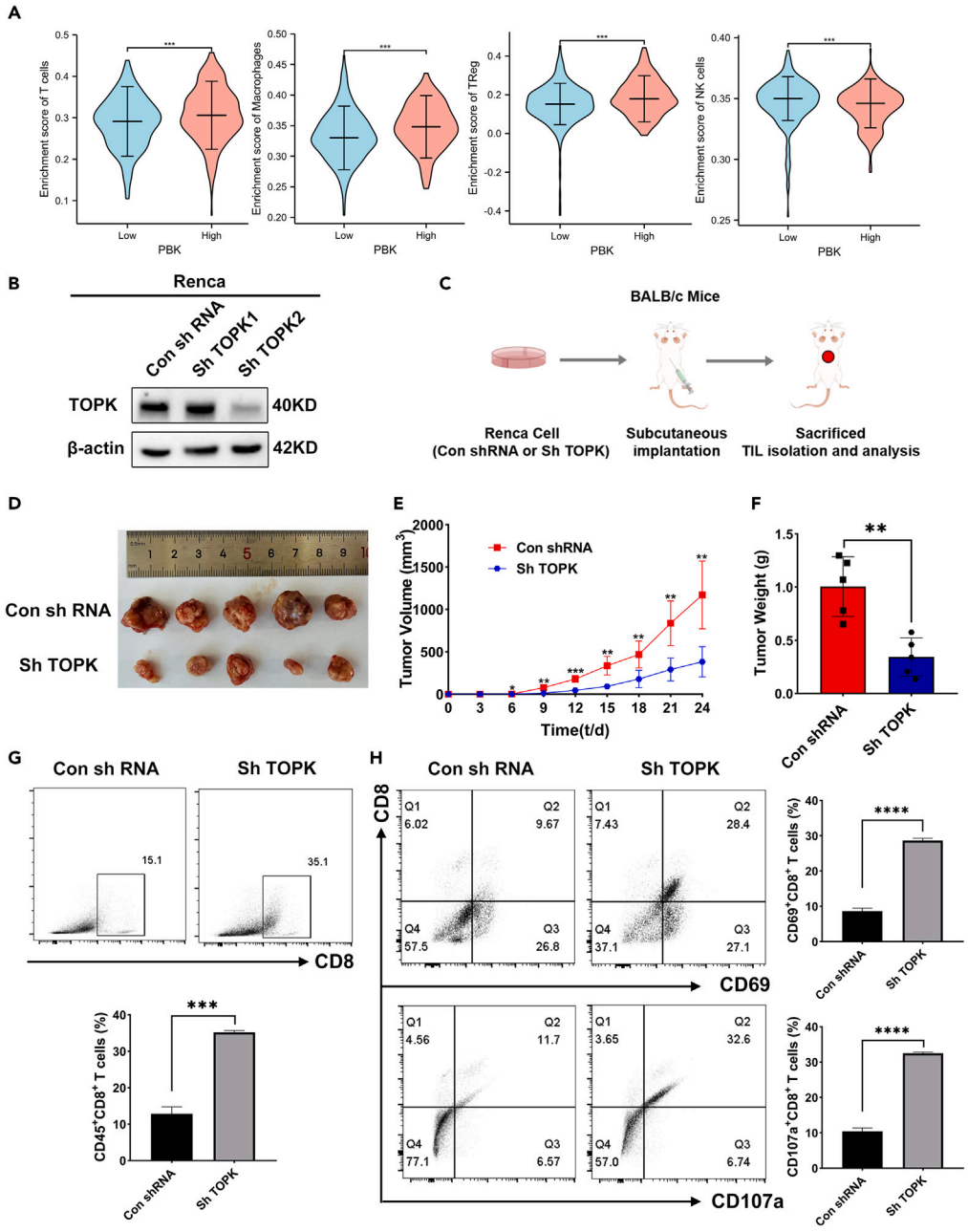

Figure 3. TOPK inhibits the function of cytotoxic CD8$^+$ T cells infiltrating in RCC tissues

(A) The relationship between TOPK and RCC-infiltrating immune cells in the TCGA database was analyzed, T cells, Treg cells, macrophages, and NK cells were shown.

(B) Knockdown of TOPK in Renca cells and TOPK expression was analyzed by immunoblot analysis.

(C) Schematic protocols displaying control or TOPK-KD Renca cells were injected subcutaneously into the back of wild BALB/c mice, respectively.

(D–E) Representative images of mouse tumors(D), tumor growth curves(E), and tumor weight (F) were shown. Tumors were measured at specified time points and dissected at the endpoint (n = 5).

(G–H) Representative images and statistical results of tumor-infiltrating lymphocytes (n = 5). The cell surface was stained with antibodies against CD8(G), CD69 and CD107a (H). Data are expressed as mean ± SD. *p < 0.05, **p < 0.01, ***p < 0.001, ns, not significant. See also Figure S2.

finding was made that the percentage of $CD8^+$ T cells expressing PD-1 decreased (Figure S2A). This was also confirmed in our *in vitro* culture experiments using conditioned medium derived from TOPK overexpression and knockdown RCC cells (Figure S2B), suggesting that TOPK may affect the secretion of certain substances by RCC cells and thus affect the expression of PD-1 on T cells. These results indicate that TOPK can inhibit the infiltration of $CD8^+$ T cells in the RCC but also significantly inhibit the activation of $CD8^+$ T cells and promote the expression of the inhibitory factor PD-1 in $CD8^+$ T cells, thereby promoting RCC tumorigenesis and immune escape.

TOPK is positively correlated with PD-L1 expression in RCC

Next, we explored the correlation between TOPK and PD-L1 expression. First, we found knockdown of TOPK in 786-O cells resulted in the downregulation of PD-L1 expression (Figure 4A). Flow cytometry detection of PD-L1 expression on the cell surface showed the same results (Figures 4B and 4C). Also, the overexpression of TOPK in Caki-1 cells resulted in the upregulation of PD-L1 expression (Figure 4D). Meanwhile, the immunoblotting and immunohistochemical staining of the above mouse tumor tissues (Figure 3C) showed that compared with the control group, a decrease of TOPK and PD-L1 expression was found in the subcutaneous tumor of the mice injected with TOPK-KD cells (Figures 4E and 4F).

Finally, we used human tissue microarrays containing 90 patients with RCC, all with cancerous and paracancerous tissues, for further verification. The results of tissue immunohistochemical staining showed that the expression level of TOPK in cancer tissues was consistent with the expression of PD-L1(Figures 4G–4I). Taken together, our results further confirmed that there is a positive association between the expression of TOPK and PD-L1 in RCC.

In RCC, the positive feedback loop between TOPK and ERK2 promotes PD-L1 expression

The positive feedback loop between TOPK and ERK2 is an important mechanism for the cancer-promoting function of TOPK.[22] Other studies have shown that ERK2 can promote the expression of PD-L1.[23] Therefore, we verified the possibility that TOPK regulates PD-L1 expression through ERK2. ERK2 expression was decreased after TOPK knockdown and increased after overexpression, indicating that TOPK can positively regulate ERK2 expression in RCC (Figures 5A and 5B). Because TOPK and ERK2 are protein kinases whose actions depend on phosphorylation levels, we next explored whether their phosphorylation levels affect PD-L1 expression. Human epidermal growth factor (EGF) is well-established as a potent MAPK pathway activator with significant activation of TOPK and ERK2.[22,24] Accordingly, we chose EGF as an activator of TOPK and ERK2. The results showed that TOPK knockdown significantly decreased the expression levels of ERK2 and PD-L1, while the phosphorylation levels of TOPK and ERK2 and the expression of PD-L1 subsequently increased after EGF stimulation (Figures 5C, and S3A). The opposite result was observed after TOPK overexpression. In addition, after ERK2 activation was inhibited by SCH772984, a potent inhibitor of ERK2 activation,[25] PDL1 expression was subsequently reduced(Figures 5D, and S3B). These results illustrate that the phosphorylation levels of TOPK and ERK2 significantly affect the expression of PD-L1. Although the use of ERK2 inhibitors resulted in the downregulation of PD-L1 expression, this still does not prove that ERK2 is the key molecule mediating TOPK regulation of PD-L1, given that SCH772984 could inhibit ERK2 activation along with TOPK activation.

We then constructed ERK2 knockout cell lines and did further studies. It was found that the knockout of ERK2 slightly downregulated the expression of TOPK, which substantiated the positive feedback loop of TOPK-ERK2 in RCC. (Figures 5E and 5F). After ERK2 knockout, we overexpressed TOPK to verify whether TOPK could upregulate PD-L1 in the absence of ERK2. The results showed that the expression level of PDL1 decreased with the knockout of ERK2, and after overexpression of TOPK, ERK2 did not increase again, but the expression of PDL1 increased subsequently, which was more obvious after EGF stimulation, suggesting that TOPK can regulate PDL1 expression, even in the absence of ERK2 (Figures 5G–H, and S3C–S3D). The above results indicate that ERK2 plays an important role in the regulatory effect of TOPK on PD-L1, and this regulatory relationship is closely related to the activation of TOPK and ERK2. However, the effect of TOPK on PD-L1 was still observed after ERK2 deletion, suggesting that although TOPK can affect PD-L1 expression by influencing the expression and activation of ERK2, this mechanism is not unique, and other regulatory mechanisms may affect the effect of TOPK on PD-L1.

TOPK promotes PD-L1 expression in RCC by enhancing TGF-β/Smad pathway activity

Transforming growth factor β(TGF-β) pathway is an important pathway affecting tumor immunity.[26] It has been established that the recruitment of *p*-Smad2/3 can significantly increase PD-L1 expression and

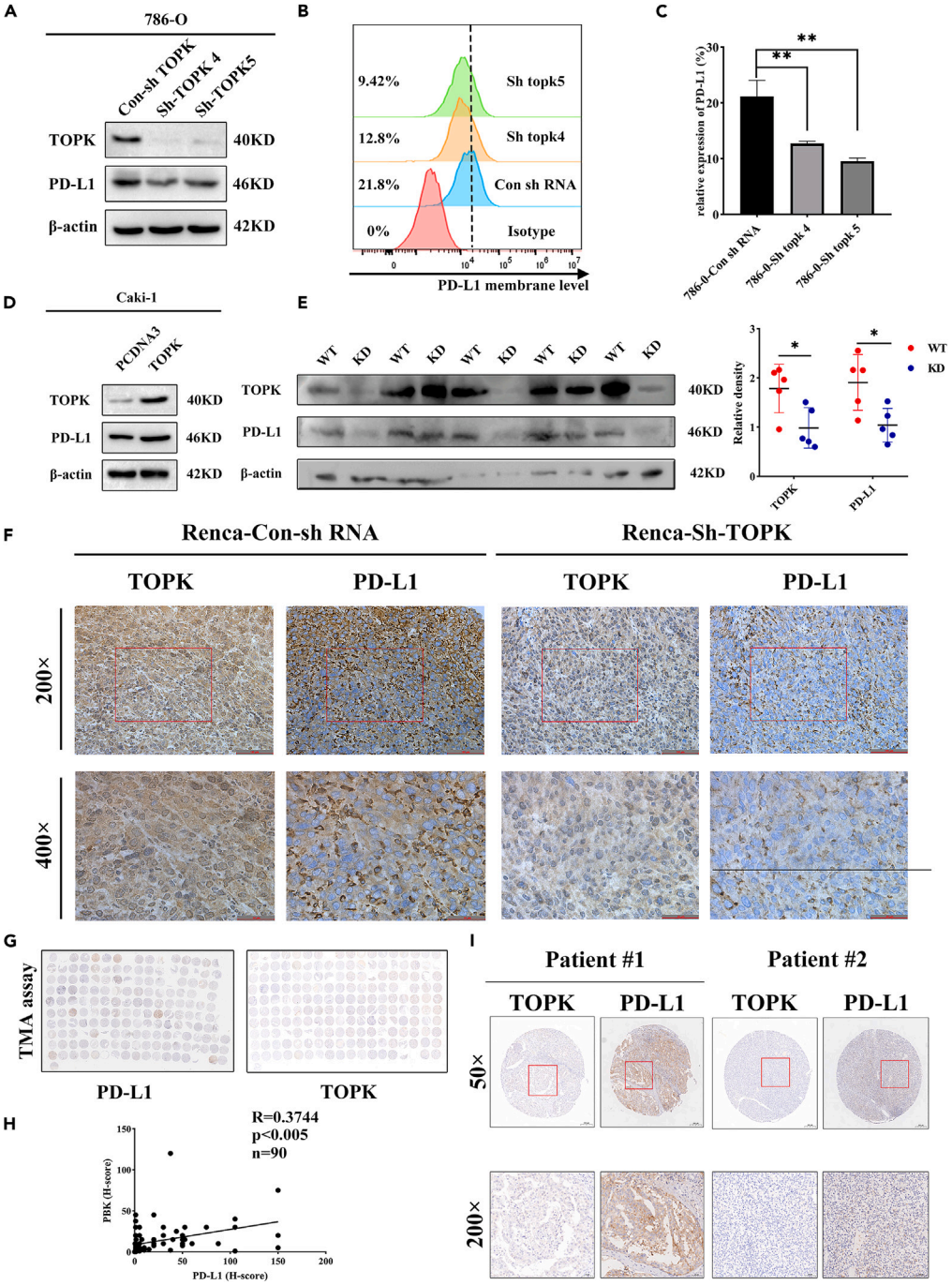

Figure 4. TOPK is positively correlated with PD-L1 expression in RCC

(A) TOPK and PD-L1 expression were detected in TOPK knockdown 786-O cells by immunoblot analysis.

(B) PD-L1 expression on the cell surface was also examined by flow cytometry, and significances were analyzed (C).

(D) TOPK and PD-L1 expression were detected in TOPK overexpressing caki-1 cells by immunoblot analysis.

(E) TOPK expression in the above mouse tumors was detected by immunoblot analysis, and significances were analyzed.

(F)The expression of TOPK and PD-L1 in mouse tumor tissues was determined by IHC. Representative views of IHC staining of TOPK and PD-L1 were presented (×200 up; ×400 down), Scale bar, 100μm or 50μm.

(G–H) IHC staining of TOPK and PD-L1 in a tissue microarray and statistical results (n = 90).

(I) Representative images of two groups of relatively high and low expression. Data are expressed as mean ± SD. *p < 0.05, **p < 0.01, ***p < 0.001, ns, not significant.

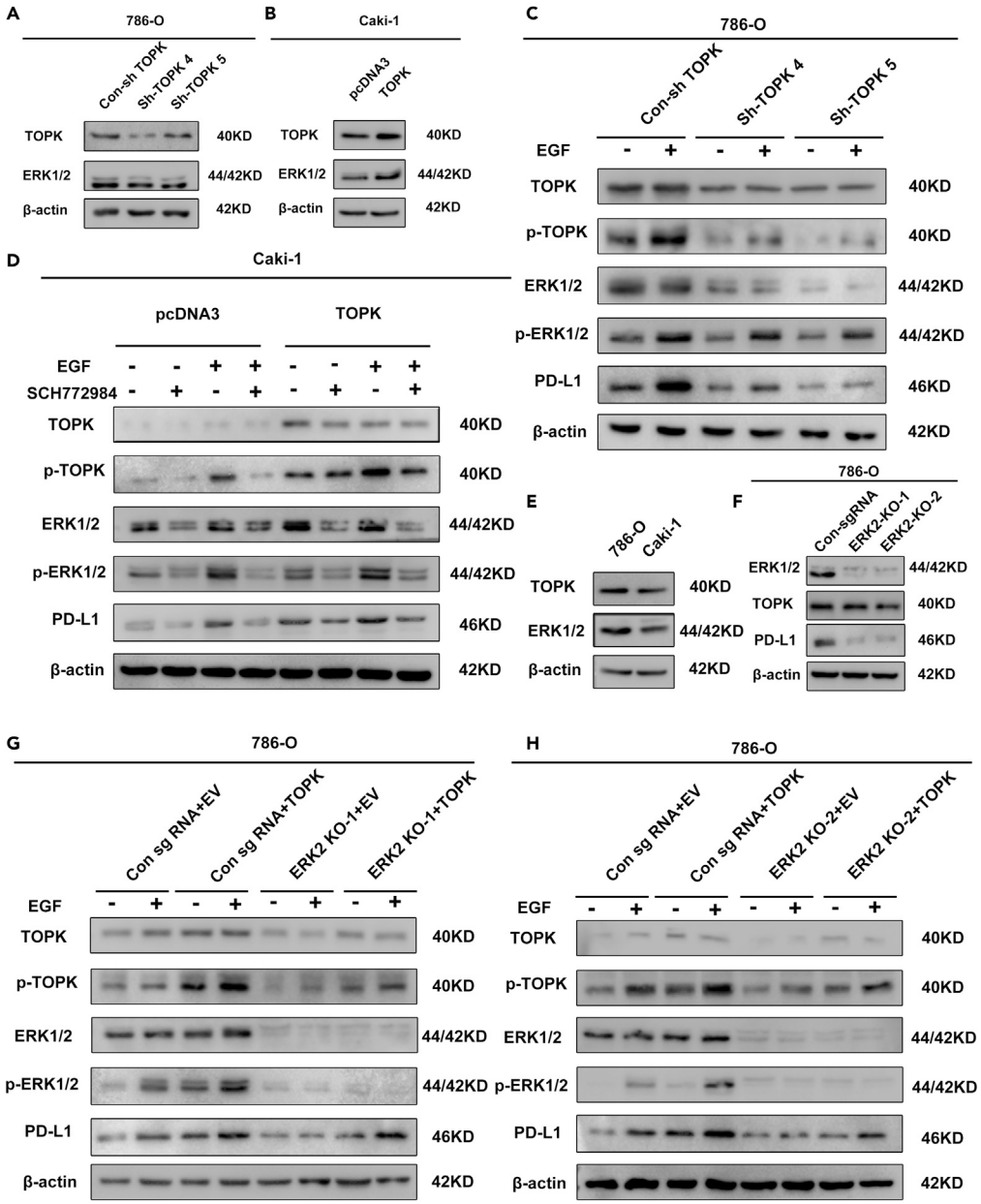

Figure 5. In RCC, the positive feedback loop between TOPK and ERK2 promotes PD-L1 expression

The expression of different proteins in different cells was detected by immunoblot analysis.

(A–B) Detection of ERK1/2 expression after TOPK knockdown or overexpression in 786-O(A) and Caki-1 cells(B), respectively.

(C) The expression of TOPK, *p*-TOPK(Thr9), ERK1/2, *p*-ERK1/2(Thr202/Tyr204), and PD-L1 was detected in TOPK knockdown 786-O cells with or without EGF treatment (40 ng/mL, 15min).

(D) The expression of TOPK, *p*-TOPK(Thr9), ERK1/2, *p*-ERK1/2(Thr202/Tyr204), and PD-L1 was detected in TOPK overexpressing Caki-1 cells treated with EGF (40 ng/mL, 15min) or SCH772984 (5nM, 24h), respectively or in combination.

(E) Expression of TOPK and ERK1/2 in 786-O and Caki-1 cells was detected.

(F) Knockout of ERK2 in 786-O cells, TOPK, ERK1/2 and PD-L1 expression were detected.

(G–H) Overexpression of TOPK in ERK2 knockout 786-O cells with or without EGF treatment (40 ng/ml, 15min), TOPK, *p*-TOPK(Thr9), ERK1/2, *p*-ERK1/2(Thr202/Tyr204), and PD-L1 was detected. See also Figure S3.

thus promote tumor immune evasion in metastatic lung adenocarcinoma.[27] Also, TOPK was shown to regulate the transcription of molecules downstream of the TGF-β/Smad pathway.[28] Therefore, we investigated whether TOPK affects PD-L1 expression and the development of immune evasion in RCC by affecting the TGF-β/Smad pathway. We found that TOPK promotes the expression of Smad4, a key molecule of the TGF-β pathway, and could bind to it (Figures 6A–6C). TGF-β1 stimulation promoted endogenous TOPK expression and phosphorylation as well as the phosphorylation of Smad2/3 and Smad4. The phosphorylation of these key molecules was accompanied by increased PD-L1 expression, which at least indicated that TGF-β1 had a significant effect on PD-L1 expression (Figure 6D). After TOPK knockdown, Smad2/3, Smad4 and PD-L1 expression were reduced (Figures 6E, and S4A), while the opposite was observed after overexpression (Figures 6F, and S4B). To verify the role of TOPK phosphorylation in this process, OTS964, a potent TOPK inhibitor, was used to inhibit TOPK phosphorylation. Although TOPK overexpression promoted the expression of Smad2/3, Smad4, and TGF-β1 further promoted their activation as well as PD-L1 expression, inhibition of TOPK activation resulted in a significant decrease in their phosphorylation levels, accompanied by a decrease in PD-L1, indicating that TOPK activation is essential for TGF-β/Smad pathway activity and PD-L1 expression (Figures 6G, and S4C).

These results suggest that the TGF-β/Smad pathway regulates PD-L1 expression in RCC, and this regulatory relationship correlates with the pathway's activity. The presence and activation of TOPK could significantly promote the phosphorylation levels of Smad2/3 and Smad4, which increased the overall activity of the pathway. Moreover, the direct binding effect of TOPK to Smad4 indicated its close association with this pathway. In conclusion, TOPK is essential for the TGF-β/Smad pathway and promotes PD-L1 expression in RCC through this mechanism.

TOPK inhibition significantly enhances anti-PD-L1 treatment efficacy in RCC

Next, we verified the effects of TOPK inhibitor and anti-PD-L1 treatment alone or in combination on subcutaneous tumors in mice. We first injected wild-type Renca cell line subcutaneously into the back of BALB/c mice, and when the tumor volume reached 50–100 mm^3, the mice were randomly divided into four groups (Figure 7A). Mice treated with OTS964 (TOPK inhibitor) or anti-PD-L1 alone exhibited reduced tumor volume compared to the control group, while the reduction in tumor volume was more pronounced in mice receiving combination treatment (Figure 7B). At the same time, there was no difference in body weight change among the four groups of mice (Figure 7C). Analysis of tumor-infiltrating immune cells by flow cytometry showed that mice treated with OTS964 or anti-PD-L1 alone had increased numbers of tumor-infiltrating $CD8^+$ T cells compared to the control group, while the combination treatment group yielded a more significant effect (Figure 7E). We next evaluated the activation of these T cells by analyzing the percentage of $CD8^+$ T cells expressing CD107a and CD69. The results showed that tumor-infiltrating $CD8^+$ T cells in mice treated with OTS964 or anti-PD-L1 alone exhibited increased expression of CD107a and CD69 compared to the control group, while the combination treatment group expressed more, implying more infiltration of activated $CD8^+$ T cells (Figure 7F). Hematoxylin and Eosin (HE) staining of the liver and kidney in all mice was conducted to evaluate the safety of OTS964 and anti-PD-L1 *in vivo* experiments (Figure S7A). As expected, there is no difference in body weight changes in mice, and the comprehensive analysis of HE staining results indicates that at least to some extent, the two drugs are relatively safe for use *in vivo* experiments (Figures 7C, and S5). These results suggested that the combination of TOPK inhibition and anti-PD-L1 treatment exerted a greater tumor-suppressive effect, which was achieved by promoting the infiltration of $CD8^+$ T cells and enhancing their activity. TOPK inhibition significantly improved the sensitivity of anti-PD-L1 treatment in RCC.

DISCUSSION

The occurrence of tumor immune evasion is reportedly a key mechanism that facilitates tumor progression.[29] During the interaction between immune cells and tumor cells, alterations in some key factors may deprive the immune system of its inhibitory function, which inevitably promotes tumor growth.[30] It is well-established that PD-1/PD-L1 plays an important role.[31] In this respect, the binding of PD-L1 expressed by tumor cells to PD-1 on the surface of T cells inhibits T cell function, which is thought to be the main mechanism by which tumor immune evasion occurs.[32] However, the expression of PD-L1 by tumor cells is regulated by various factors within the tumor cells.[33] Accordingly, even in the same tumor, PD-L1 may be expressed at different levels, directly affecting the efficacy of clinical anti-PD-L1 therapy.[34]

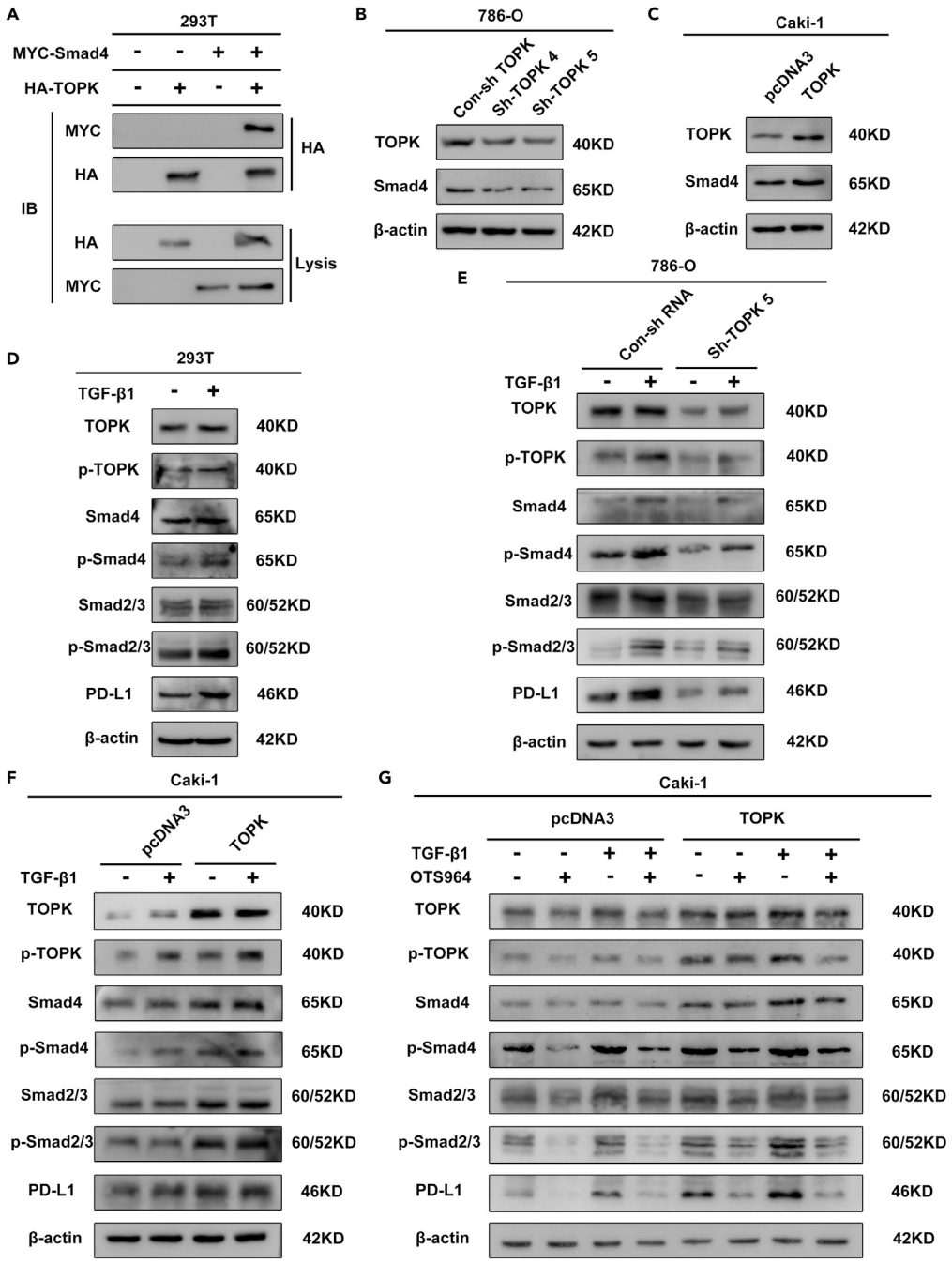

Figure 6. TOPK promotes PD-L1 expression in RCC by enhancing TGF-β/Smad pathway activity

The expression of different proteins in different cells was detected by immunoblot analysis.

(A) Detection of TOPK binding to Smad4 by immunoprecipitation.

(B-C) The expression of TOPK and Smad4 in TOPK knockdown 786-O cells(B) and overexpressed Caki-1 cells(C) were detected, respectively.

(D) The expression of TOPK, *p*-TOPK(Thr9), Smad4, *p*-Smad4 (Thr276), Smad2/3, *p*-Smad2/3 (S465, 467/S423, 425), and PD-L1 was detected in 293T cells with or without TGF-β1 (5 ng/ml, 2h).

(E-F) The expression of TOPK, *p*-TOPK(Thr9), Smad4, *p*-Smad4 (Thr276), Smad2/3, *p*-Smad2/3 (S465, 467/S423, 425), and PD-L1 was detected in TOPK knockdown (E) or overexpressed cells(F) with or without TGF-β1 (5 ng/ml, 2h). (G) Expression of TOPK, *p*-TOPK(Thr9), Smad4, *p*-Smad4 (Thr276), Smad2/3, *p*-Smad2/3 (S465, 467/S423, 425), and PD-L1 was detected in TOPK overexpressing cells alone or in combination with TGF-β1 (5 ng/mL, 2h) and OTS964 (10nM, 24h). See also Figure S4.

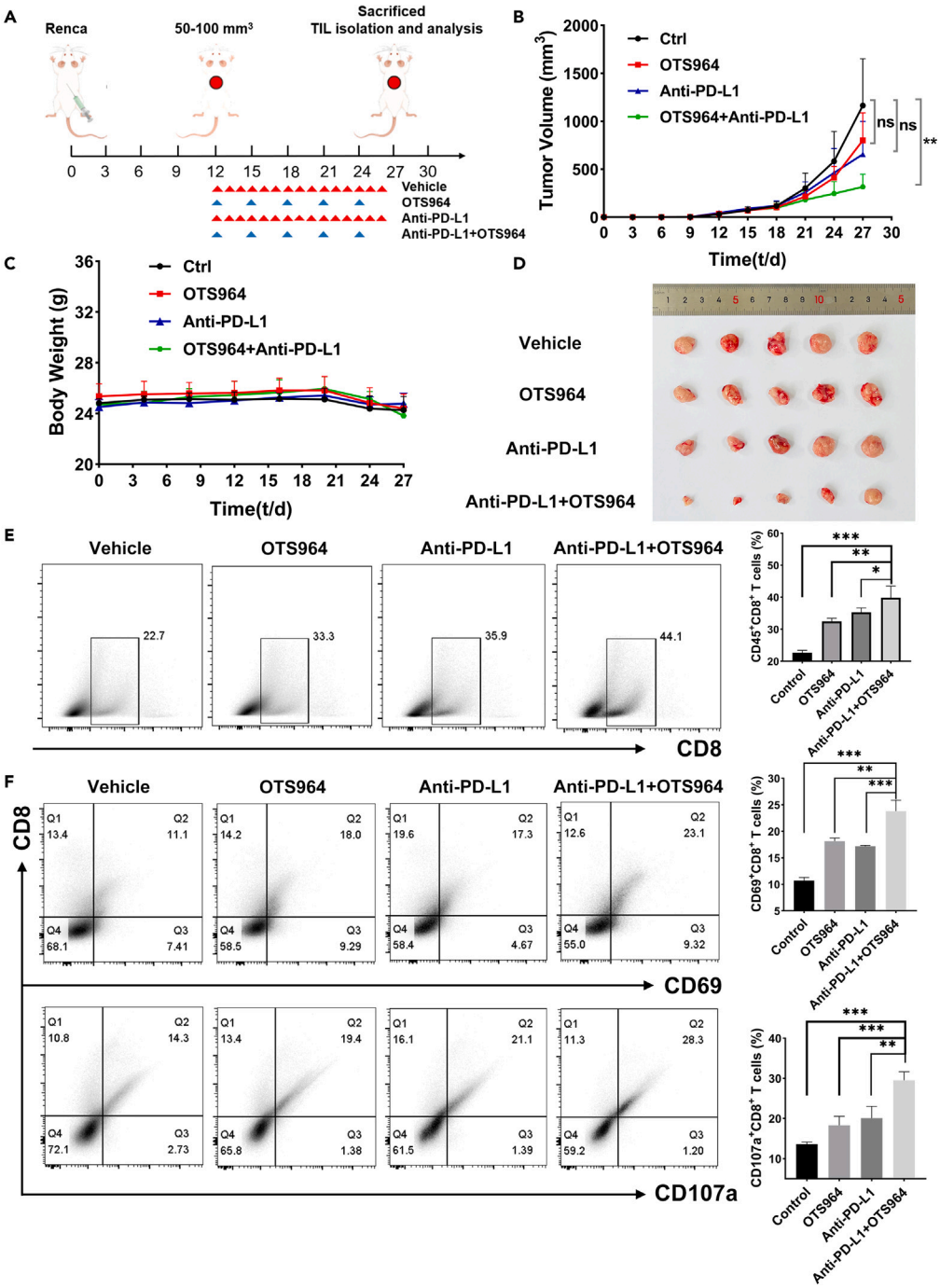

Figure 7. TOPK inhibition significantly enhances anti-PD-L1 treatment efficacy in RCC

(A) The process of animal experimentation and treatment strategies were demonstrated.

(B–D) tumor growth curves(B), Body weights(C), and representative images of tumors(D) from four groups of mice with different treatment regimens were visualized(n = 5).

(E–F) Representative images and statistical results of tumor-infiltrating lymphocytes (n = 5). Cell surface was stained with antibodies against CD8(E), as well as CD69 and CD107a(F). Data are expressed as mean ± SD. *p < 0.05, **p < 0.01, ***p < 0.001, ns, not significant. See also Figure S5.

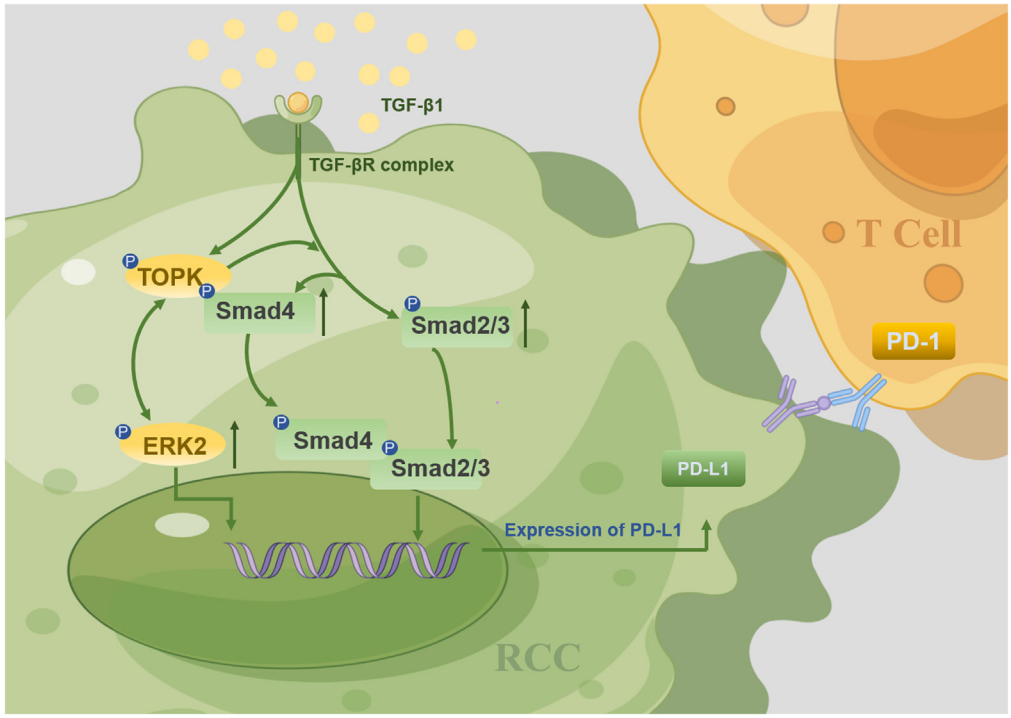

Figure 8. A model depicting the expression of PD-L1 regulated by TOPK

On the one hand, the positive feedback activation mechanism of TOPK and ERK2 promotes the expression of PD-L1 in RCC. On the other hand, TOPK not only promotes the expression of Smad2/3 and Smad4, but also can directly bind to smad4. The stimulation of TGF-β1 caused phosphorylation of TOPK, which significantly enhanced the activation of TGF-β/Smad pathway and promoted the expression of PD-L1. Therefore, TOPK is essential for the TGF-β/Smad pathway and can significantly amplify the effects of this pathway.

TOPK is widely acknowledged to be highly expressed in various tumors, while expressed only in a few normal cells or tissues, such as testis,[35] sperm, neural precursor cells in the subventricular zone of the adult brain, and in a few ischemic tissues, including heart, brain and kidney.[36] This feature allows it to act as an independent tumor risk and prognostic factor. As a protein kinase, TOPK exerts its pro-cancer effects mainly through the activation of the MAPK pathway, especially ERK2.[18,22] At the same time, it can promote tumor progression through other mechanisms. Therefore, disabling TOPK represents a valuable therapeutic approach. In the present study, we found that TOPK could affect the infiltration of $CD8^+$ T cells in RCC and their activation, providing compelling evidence that TOPK can regulate immune escape from RCC (Figure 3). Meanwhile, TOPK increased the expression level of PDL1 in RCC, improving the current understanding of the mechanism of PD-L1 expression regulation in RCC and offering the possibility to improve the efficacy of anti-PD-L1 therapy. Indeed, our results provide hitherto undocumented evidence that simultaneous inhibition of TOPK and PD-L1 yielded a potent inhibitory effect on RCC, with increased $CD8^+$ T cell infiltrates and functional recovery (Figure 7).

Mechanistically, we found that the positive feedback loop of TOPK and ERK2 also existed in RCC and could promote PD-L1 expression. However, ERK2 was not necessary for TOPK to regulate PD-L1 expression, suggesting that the regulatory mechanisms of TOPK on PD-L1 may be heterogeneous (Figures 5 and 8). Meanwhile, we found that TOPK plays a critical role in the TGF-β/Smad pathway. Although previous studies have reported a connection between TOPK and TGF-β/Smad pathway,[37] our findings suggest that TOPK promotes the protein expression of Smad2/3 and Smad4 and functions in direct binding with Smad4. Stimulation of TGF-β1 enables TOPK activation, which leads to the overall activation of the TGF-β/Smad pathway, because the phosphorylation levels of Smad2/3 and Smad4 were significantly higher. In contrast, silencing or inhibition of TOPK resulted in significantly lower expression levels and activation levels of Smad2/3 and Smad4 and, at the same time, affected the PD-L1 expression mediated by the TGF-β/Smad pathway (Figures 6 and 8). Therefore, TOPK is essential for the TGF-β/Smad pathway, and its presence undoubtedly reinforces the pro-cancer effect of this pathway.

Currently, several inhibitors have been proven to be effective in inhibiting TOPK activity and exerting antitumor effects both *in vitro* and *in vivo*, including HI-TOPK-032,[38] OTS514/OTS964,[39] and ADA-07.[40] However, among these inhibitors, OTS964, a derivative of OTS514, was shown to have a more efficient inhibitory effect and an ability to overcome the weight loss because of OTS514-induced blood toxicity.[41] Although the free form of OTS964 still causes some degree of blood toxicity, new technologies such as liposome delivery forms and nanocarriers technology are well able to avoid it.[39,42] These features are pivotal for the *in vivo* application of OTS964 and also significantly contribute to the use of TOPK inhibitors in the clinic to improve antitumor treatment efficacy.

Limitations of the study

However, what we found may only be the tip of the iceberg regarding its mechanism of action, and more studies are warranted to explore the connection and regulatory mechanism between TOPK and TGF-β/Smad pathway, such as the effect of TOPK on the stability and complex formation of Smad2/3 and Smad4. Although we found that the expression level of TOPK in RCC can influence the expression of PD-1 on T cells, its mechanism of action still needs further exploration, and we speculate that this may be achieved by promoting the secretion of certain cytokines or extracellular vesicles by TOPK in RCC cells. In addition, we only studied the antitumor effect of the combination of TOPK inhibitor and anti-PD-L1 for 27 days, while studying the effect over a longer period of time would be more useful to clarify the clinical application of TOPK inhibitors. These are the directions we need to work on in the future and will be a further elucidation of the effect of TOPK on tumor immunity. Overall, our study illustrates that TOPK can play an important role as a potential molecular target in the diagnosis, treatment and prognosis assessment of RCC.

STAR★METHODS

Detailed methods are provided in the online version of this paper and include the following:

- KEY RESOURCES TABLE
- RESOURCE AVAILABILITY
  - Lead contact
  - Materials availability
  - Data and code availability
- EXPERIMENTAL MODEL AND SUBJECT DETAILS
  - Mice
- METHOD DETAILS
  - Transient transfection and establishment of stably transfected cell lines
  - MTT cell proliferation assay
  - EDU proliferation assay
  - Transwell cell migration assay
  - Wound healing experiment
  - Preparation of CM and Jurkat cell culture experiment
  - Immunoblotting and immunoprecipitation
  - Establishment of mouse tumor models
  - Mouse tumor CTL isolation and flow cytometry experiments
  - Immunohistochemistry
- QUANTIFICATION AND STATISTICAL ANALYSIS
  - Statistical analysis

SUPPLEMENTAL INFORMATION

Supplemental information can be found online at https://doi.org/10.1016/j.isci.2023.107185.

ACKNOWLEDGMENTS

This work was supported by the Natural Science Foundation of China [81972373]; the Scientific Research Foundation for Advanced Talents, Xiang'an Hospital of Xiamen University [PM201809170001]; and a Research Fund of Fujian Key Laboratory of Precision Diagnosis and Treatment in Breast Cancer & Xiamen Key Laboratory of Endocrine-Related Cancer Precision Medicine. We also thank Figdraw (www.figdraw.com) for the assistance in creating Graphical abstract and Figure 8.

AUTHOR CONTRIBUTIONS

C.S. conceived the project. J.L. and H.S. designed and supervised all experiments, edited the manuscript. M.F. helped in animal experiments. Z.Z. helped in WB experiments. C.X. and K.Y. helped with bioinformatics analysis. Y.L. and Z.X. involved in analyzing the histology and histopathology. Y.B., J.Z., Y.Z., and Z.S. involved in interpreting and analyzing the data. All authors have seen and approved the manuscript being submitted.

DECLARATION OF INTERESTS

The authors declare no competing interests.

Received: March 26, 2023
Revised: May 8, 2023
Accepted: June 16, 2023
Published: June 20, 2023

REFERENCES

1. Cairns, P. (2010). Renal cell carcinoma. Cancer Biomark. *9*, 461–473. https://doi.org/10.3233/CBM-2011-0176.

2. Hsieh, J.J., Purdue, M.P., Signoretti, S., Swanton, C., Albiges, L., Schmidinger, M., Heng, D.Y., Larkin, J., and Ficarra, V. (2017). Renal cell carcinoma. Nat. Rev. Dis. Primers *3*, 17009. https://doi.org/10.1038/nrdp.2017.9.

3. Shuch, B., Amin, A., Armstrong, A.J., Eble, J.N., Ficarra, V., Lopez-Beltran, A., Martignoni, G., Rini, B.I., and Kutikov, A. (2015). Understanding pathologic variants of renal cell carcinoma: distilling therapeutic opportunities from biologic complexity. Eur. Urol. *67*, 85–97. https://doi.org/10.1016/j.eururo.2014.04.029.

4. Siva, S., Kothari, G., Muacevic, A., Louie, A.V., Slotman, B.J., Teh, B.S., and Lo, S.S. (2017). Radiotherapy for renal cell carcinoma: renaissance of an overlooked approach. Nat. Rev. Urol. *14*, 549–563. https://doi.org/10.1038/nrurol.2017.87.

5. Lilleby, W., and Fosså, S.D. (2005). Chemotherapy in metastatic renal cell cancer. World J. Urol. *23*, 175–179. https://doi.org/10.1007/s00345-004-0469-x.

6. Kunath, F., Schmidt, S., Krabbe, L.-M., Miernik, A., Dahm, P., Cleves, A., Walther, M., and Kroeger, N. (2017). Partial nephrectomy versus radical nephrectomy for clinical localised renal masses. Cochrane Database Syst. Rev. *5*, CD012045. https://doi.org/10.1002/14651858.CD012045.pub2.

7. Husillos Alonso, A., Carbonero García, M., and González Enguita, C. (2015). Is there a role for systemic targeted therapy after surgical treatment for metastases of renal cell carcinoma? World J. Nephrol. *4*, 254–262. https://doi.org/10.5527/wjn.v4.i2.254.

8. Ross, K., and Jones, R.J. (2017). Immune checkpoint inhibitors in renal cell carcinoma. Clin. Sci. *131*, 2627–2642. https://doi.org/10.1042/CS20160894.

9. Bedke, J., Albiges, L., Capitanio, U., Giles, R.H., Hora, M., Lam, T.B., Ljungberg, B., Marconi, L., Klatte, T., Volpe, A., et al. (2021). The 2021 Updated European Association of Urology Guidelines on Renal Cell Carcinoma: Immune Checkpoint Inhibitor-based Combination Therapies for Treatment-naive Metastatic Clear-cell Renal Cell Carcinoma Are Standard of Care. Eur. Urol. *80*, 393–397. https://doi.org/10.1016/j.eururo.2021.04.042.

10. Ljungberg, B., Albiges, L., Abu-Ghanem, Y., Bedke, J., Capitanio, U., Dabestani, S., Fernández-Pello, S., Giles, R.H., Hofmann, F., Hora, M., et al. (2022). European Association of Urology Guidelines on Renal Cell Carcinoma: The 2022 Update. Eur. Urol. *82*, 399–410. https://doi.org/10.1016/j.eururo.2022.03.006.

11. Lombardi, P., Filetti, M., Falcone, R., Di Bidino, R., Iacovelli, R., Ciccarese, C., Bria, E., Tortora, G., Scambia, G., and Daniele, G. (2022). New first-line immunotherapy-based combinations for metastatic renal cell carcinoma: A systematic review and network meta-analysis. Cancer Treat Rev. *106*, 102377. https://doi.org/10.1016/j.ctrv.2022.102377.

12. Sharma, R., Kadife, E., Myers, M., Kannourakis, G., Prithviraj, P., and Ahmed, N. (2021). Determinants of resistance to VEGF-TKI and immune checkpoint inhibitors in metastatic renal cell carcinoma. J. Exp. Clin. Cancer Res. *40*, 186. https://doi.org/10.1186/s13046-021-01961-3.

13. Morad, G., Helmink, B.A., Sharma, P., and Wargo, J.A. (2021). Hallmarks of response, resistance, and toxicity to immune checkpoint blockade. Cell *184*, 5309–5337. https://doi.org/10.1016/j.cell.2021.09.020.

14. Gaudet, S., Branton, D., and Lue, R.A. (2000). Characterization of PDZ-binding kinase, a mitotic kinase. Proc. Natl. Acad. Sci. USA *97*, 5167–5172. https://doi.org/10.1073/pnas.090102397.

15. Abe, Y., Matsumoto, S., Kito, K., and Ueda, N. (2000). Cloning and expression of a novel MAPKK-like protein kinase, lymphokine-activated killer T-cell-originated protein kinase, specifically expressed in the testis and activated lymphoid cells. J. Biol. Chem. *275*, 21525–21531. https://doi.org/10.1074/jbc.M909629199.

16. Herbert, K.J., Ashton, T.M., Prevo, R., Pirovano, G., and Higgins, G.S. (2018). T-LAK cell-originated protein kinase (TOPK): an emerging target for cancer-specific therapeutics. Cell Death Dis. *9*, 1089. https://doi.org/10.1038/s41419-018-1131-7.

17. Herbert, K.J., Puliyadi, R., Prevo, R., Rodriguez-Berriguete, G., Ryan, A., Ramadan, K., and Higgins, G.S. (2021). Targeting TOPK sensitises tumour cells to radiation-induced damage by enhancing replication stress. Cell Death Differ. *28*, 1333–1346. https://doi.org/10.1038/s41418-020-00655-1.

18. Sun, H., Zheng, J., Xiao, J., Yue, J., Shi, Z., Xuan, Z., Chen, C., Zhao, Y., Tang, W., Ye, S., et al. (2022). TOPK/PBK is phosphorylated by ERK2 at serine 32, promotes tumorigenesis and is involved in sorafenib resistance in RCC. Cell Death Dis. *13*, 450. https://doi.org/10.1038/s41419-022-04909-3.

19. Lee, D.-H., Jeong, Y.-J., Won, J.-Y., Sim, H.-I., Park, Y., and Jin, H.-S. (2022). PBK/TOPK Is a Favorable Prognostic Biomarker Correlated with Antitumor Immunity in Colon Cancers. Biomedicines *10*, 299. https://doi.org/10.3390/biomedicines10020299.

20. Feng, T., Zhang, Y., Ling, S., Xu, C., Lyu, Y., Lu, T., Liu, X., Ying, L., Wan, Y., Zhong, H., and Su, D. (2021). PDZ Binding Kinase/T-LAK Cell-Derived Protein Kinase Plays an Oncogenic Role and Promotes Immune Escape in Human Tumors. J. Oncol. *2021*, 8892479. https://doi.org/10.1155/2021/8892479.

21. Qin, G., Wang, X., Ye, S., Li, Y., Chen, M., Wang, S., Qin, T., Zhang, C., Li, Y., Long, Q., et al. (2020). NPM1 upregulates the transcription of PD-L1 and suppresses T cell activity in triple-negative breast cancer. Nat. Commun. *11*, 1669. https://doi.org/10.1038/s41467-020-15364-z.

22. Zhu, F., Zykova, T.A., Kang, B.S., Wang, Z., Ebeling, M.C., Abe, Y., Ma, W.-Y., Bode, A.M., and Dong, Z. (2007). Bidirectional signals transduced by TOPK-ERK interaction

increase tumorigenesis of HCT116 colorectal cancer cells. Gastroenterology *133*, 219–231. https://doi.org/10.1053/j.gastro.2007.04.048.

23. Zhu, Y., Gu, L., Lin, X., Zhou, X., Lu, B., Liu, C., Lei, C., Zhou, F., Zhao, Q., Prochownik, E.V., and Li, Y. (2021). USP19 exacerbates lipogenesis and colorectal carcinogenesis by stabilizing ME1. Cell Rep. *37*, 110174. https://doi.org/10.1016/j.celrep.2021.110174.

24. Sheng, W., Shi, X., Lin, Y., Tang, J., Jia, C., Cao, R., Sun, J., Wang, G., Zhou, Z., Dong, M., et al. (2020). Musashi2 promotes EGF-induced EMT in pancreatic cancer via ZEB1-ERK/MAPK signaling. J. Exp. Clin. Cancer Res. *39*, 16. https://doi.org/10.1186/s13046-020-1521-4.

25. Morris, E.J., Jha, S., Restaino, C.R., Dayananth, P., Zhu, H., Cooper, A., Carr, D., Deng, Y., Jin, W., Black, S., et al. (2013). Discovery of a novel ERK inhibitor with activity in models of acquired resistance to BRAF and MEK inhibitors. Cancer Discov. *3*, 742–750. https://doi.org/10.1158/2159-8290.CD-13-0070.

26. Sanjabi, S., Oh, S.A., and Li, M.O. (2017). Regulation of the Immune Response by TGF-β: From Conception to Autoimmunity and Infection. Cold Spring Harb. Perspect. Biol. *9*, a022236. https://doi.org/10.1101/cshperspect.a022236.

27. Jang, H.-R., Shin, S.-B., Kim, C.-H., Won, J.-Y., Xu, R., Kim, D.-E., and Yim, H. (2021). PLK1/vimentin signaling facilitates immune escape by recruiting Smad2/3 to PD-L1 promoter in metastatic lung adenocarcinoma. Cell Death Differ. *28*, 2745–2764. https://doi.org/10.1038/s41418-021-00781-4.

28. Lee, Y.-J., Park, J.-H., and Oh, S.-M. (2020). Activation of NF-κB by TOPK upregulates Snail/Slug expression in TGF-β1 signaling to induce epithelial-mesenchymal transition and invasion of breast cancer cells. Biochem. Biophys. Res. Commun. *530*, 122–129. https://doi.org/10.1016/j.bbrc.2020.07.015.

29. Vinay, D.S., Ryan, E.P., Pawelec, G., Talib, W.H., Stagg, J., Elkord, E., Lichtor, T., Decker, W.K., Whelan, R.L., Kumara, H.M.C.S., et al. (2015). Immune evasion in cancer: Mechanistic basis and therapeutic strategies. Semin. Cancer Biol. *35* (*Suppl*), S185–S198. https://doi.org/10.1016/j.semcancer.2015.03.004.

30. Rabinovich, G.A., Gabrilovich, D., and Sotomayor, E.M. (2007). Immunosuppressive strategies that are mediated by tumor cells. Annu. Rev. Immunol. *25*, 267–296. https://doi.org/10.1146/annurev.immunol.25.022106.141609.

31. Blank, C., Kuball, J., Voelkl, S., Wiendl, H., Becker, B., Walter, B., Majdic, O., Gajewski, T.F., Theobald, M., Andreesen, R., and Mackensen, A. (2006). Blockade of PD-L1 (B7-H1) augments human tumor-specific T cell responses in vitro. Int. J. Cancer *119*, 317–327. https://doi.org/10.1002/ijc.21775.

32. Dong, H., Strome, S.E., Salomao, D.R., Tamura, H., Hirano, F., Flies, D.B., Roche, P.C., Lu, J., Zhu, G., Tamada, K., et al. (2002). Tumor-associated B7-H1 promotes T-cell apoptosis: a potential mechanism of immune evasion. Nat. Med. *8*, 793–800. https://doi.org/10.1038/nm730.

33. Pardoll, D.M. (2012). The blockade of immune checkpoints in cancer immunotherapy. Nat. Rev. Cancer *12*, 252–264. https://doi.org/10.1038/nrc3239.

34. Sun, C., Mezzadra, R., and Schumacher, T.N. (2018). Regulation and Function of the PD-L1 Checkpoint. Immunity *48*, 434–452. https://doi.org/10.1016/j.immuni.2018.03.014.

35. Fujibuchi, T., Abe, Y., Takeuchi, T., Ueda, N., Shigemoto, K., Yamamoto, H., and Kito, K. (2005). Expression and phosphorylation of TOPK during spermatogenesis. Dev. Growth Differ. *47*, 637–644. https://doi.org/10.1111/j.1440-169X.2005.00834.x.

36. Han, Z., Li, L., Huang, Y., Zhao, H., and Luo, Y. (2021). PBK/TOPK: A Therapeutic Target Worthy of Attention. Cells *10*, 371. https://doi.org/10.3390/cells10020371.

37. Lee, Y.-J., Park, J.-H., and Oh, S.-M. (2020). TOPK promotes epithelial-mesenchymal transition and invasion of breast cancer cells through upregulation of TBX3 in TGF-β1/Smad signaling. Biochem. Biophys. Res. Commun. *522*, 270–277. https://doi.org/10.1016/j.bbrc.2019.11.104.

38. Kim, D.J., Li, Y., Reddy, K., Lee, M.-H., Kim, M.O., Cho, Y.-Y., Lee, S.-Y., Kim, J.-E., Bode, A.M., and Dong, Z. (2012). Novel TOPK inhibitor HI-TOPK-032 effectively suppresses colon cancer growth. Cancer Res. *72*, 3060–3068. https://doi.org/10.1158/0008-5472.CAN-11-3851.

39. Matsuo, Y., Park, J.H., Miyamoto, T., Yamamoto, S., Hisada, S., Alachkar, H., and Nakamura, Y. (2014). TOPK inhibitor induces complete tumor regression in xenograft models of human cancer through inhibition of cytokinesis. Sci. Transl. Med. *6*, 259ra145. https://doi.org/10.1126/scitranslmed.3010277.

40. Gao, G., Zhang, T., Wang, Q., Reddy, K., Chen, H., Yao, K., Wang, K., Roh, E., Zykova, T., Ma, W., et al. (2017). ADA-07 Suppresses Solar Ultraviolet-Induced Skin Carcinogenesis by Directly Inhibiting TOPK. Mol. Cancer Ther. *16*, 1843–1854. https://doi.org/10.1158/1535-7163.MCT-17-0212.

41. Huang, H., Lee, M.-H., Liu, K., Dong, Z., Ryoo, Z., and Kim, M.O. (2021). PBK/TOPK: An Effective Drug Target with Diverse Therapeutic Potential. Cancers *13*, 2232. https://doi.org/10.3390/cancers13092232.

42. Shi, G., Cui, Y., Zhao, J., Liu, J., Wang, Y., Yang, Y., Han, J., Cheng, X., Chen, L., Yuan, Y., and Mi, P. (2023). Identifying TOPK and Hypoxia Hallmarks in Esophageal Tumors for Photodynamic/Chemo/Immunotherapy and Liver Metastasis Inhibition with Nanocarriers. ACS Nano *17*, 6193–6207. https://doi.org/10.1021/acsnano.2c07488.

STAR★METHODS

KEY RESOURCES TABLE

REAGENT or RESOURCE	SOURCE	IDENTIFIER
Antibodies		
TOPK	Cell Signaling Technology	Cat# 4942 RRID: AB_2160130
p-TOPK	Cell Signaling Technology	Cat# 4941 RRID: AB_2160132
ERK1/2	Cell Signaling Technology	Cat# 4695 RRID: AB_390779
p-ERK1/2	Cell Signaling Technology	Cat# 4370 RRID: AB_2315112
PD-L1	Cell Signaling Technology	Cat# 13684 RRID: AB_2687655
MYC-tag	Cell Signaling Technology	Cat# 2276 RRID: AB_331783
HA-tag	Cell Signaling Technology	Cat# 3724 RRID: AB_1549585
Smad4	Cell Signaling Technology	Cat# 46535 RRID: AB_2736998
Smad2/3	Cell Signaling Technology	Cat# 8685 RRID: AB_10889933
p-Smad4	Affinity Biosciences	Cat# AF8316 RRID: AB_2840378
p-Smad2/3	ABclonal	Cat# AP0548 RRID: AB_2863784
β-actin	ABclonal	Cat# AC038 RRID: AB_2863784
FITC-anti-mouse-CD45	Biolegend	Cat# 147710 RRID: AB_2563542
Percp/Cy5.5-anti-mouse-CD107a	Biolegend	Cat# 121626 RRID: AB_2572055
BV421-anti- mouse-CD69	Biolegend	Cat# 104527 RRID: AB_10900250
PE-anti-mouse-PD-1	Biolegend	Cat# 135206 RRID: AB_1877231
PE-anti-human-PD-L1	Biolegend	Cat# 329706 RRID: AB_940368
APC-anti-human-PD-1	Biolegend	Cat# 329908 RRID: AB_940475
In Vivo MAb anti-mouse PD-L1	Bio X Cell	Cat# BE0101 RRID: AB_10949073
Chemicals, peptides, and recombinant proteins		
Human TGF-β1	R&D Systems	Cat# 7754-BH
Human EGF	R&D Systems	Cat# 236-EG
OTS964	MedChemExpress	Cat# HY-12467
SCH772984	MedChemExpress	Cat# HY-50846

(*Continued on next page*)

Continued

REAGENT or RESOURCE	SOURCE	IDENTIFIER
Experimental models: Cell lines		
786-O	ATCC	CRL-1932
Caki-1	ATCC	HTB-46
ACHN	ATCC	CRL-1611
Jurkat	ATCC	TIB-152
Renca	ATCC	CRL-2947
HEK 293T	ATCC	CRL-3216
SN12C	Sun, H et al.[18]	N/A
Recombinant DNA		
Plasmid: HA-TOPK	Sino Biological	HG10729
Plasmid: MYC-Smad4	Sino Biological	HG11010
Software and algorithms		
FlowJo v10	BD	https://www.flowjo.com/
GraphPad Prism 8	Graph Pad	https://www.graphpad.com/

RESOURCE AVAILABILITY

Lead contact

Further information and requests for resources and reagents should be directed to and will be fulfilled by the lead contact: Chen Shao (cshao@xah.xmu.edu.cn).

Materials availability

This study did not generate new unique reagents.

Data and code availability

- All data reported in this paper will be shared by the lead contact upon request.
- This paper does not report original code.
- Any additional information required to reanalyze the data reported in this paper is available from the lead contact upon request.

EXPERIMENTAL MODEL AND SUBJECT DETAILS

Mice

6-8 week-old male wild-type BALB/c mice were purchased from the Xiamen University Laboratory Animal Center and were housed in a specific pathogen-free (SPF) environment at the Xiamen University Laboratory Animal Center. All animal experiments were approved by the Ethics Committee of Xiamen University School of Medicine.

METHOD DETAILS

Transient transfection and establishment of stably transfected cell lines

Caki-1 cells were used to construct TOPK overexpression cell lines, and the control PCDNA3.1 and TOPK plasmids were transfected according to the reagent instructions using lipo3000 transfection reagent (Invitrogen, USA). 48h after transfection, the transfection efficiency could be detected by RT-qPCR and Western Blot. As for constructing stably transfected cell lines, the plasmids were first transfected according to the above method, and after 48h of transfection, screening was performed using appropriate concentrations of G418 for 7-10 days.

MTT cell proliferation assay

The cell proliferation ability was measured using the MTT (thiazolyl blue) method. RCC cells with good growth in the logarithmic phase were plated in a 96-well plate at a density of 3×10^3 cells per well, and

3-5 replicate wells were set for each group. After the cells were plastered, the culture medium was replaced and selected for detection every 24h from day 0-6. 10ul of 5mg/ml MTT solution (Sigma, MO, USA) was added to each well (ready-to-use, protected from light, note that no air bubbles should be generated), and the culture was continued for 4h protected from light. 150ul of DMSO was added to each well after careful aspiration of the culture solution, placed on a shaker for 10min, and the absorbance value of each well was detected at 570nm in a microplate reader. Then the data were analyzed and processed.

EDU proliferation assay

The proliferation of RCC cells was measured using the EdU Cell Proliferation Assay Kit (Q10310-1, RiboBio, China). RCC cells were stained with 5-ethynyl-20-deoxyuridine (EdU) according to the kit instructions and photographed and recorded under a fluorescent microscope. The percentage of EdU in each field of view was quantified using ImageJ and GraphPad Prism 8.0 software for differential analysis and graphing.

Transwell cell migration assay

RCC cells in the logarithmic phase were selected and starved in serum-free RPMI-1640 medium for 6 h. The cells were digested with trypsin, centrifuged, and resuspended in serum-free RPMI-1640 medium to form a single-cell suspension. 3.5×10^4 cells were placed in the transwell plates ensuring the total amount of cell suspension was 100ul per well. 800ul of RPMI-1640 medium containing 20% fetal bovine serum was added to each well in the lower chamber of the 24-well plate, labeled, and incubated for 24h or 48h in the cell incubator. The cells were fixed in the lower chamber by adding 500ul 4% paraformaldehyde per well for 20min. The chambers were washed with PBS buffer 2-3 times and stained with 500ul 0.1% crystal violet solution per well in the lower chamber for 20min. The inner cells of the chamber were slowly wiped off with a cotton swab, and the outer wall cells were retained. The chambers were dried at room temperature and placed under a microscope for observation. 5 randomly selected fields of view were photographed under a 200× field of view. ImageJ software was used to calculate the number of cells, and GraphPad Prism 8.0 software was used to analyze the differences.

Wound healing experiment

RCC cells in the logarithmic phase were selected, and the 6-well plates were spread with 1×10^6 cells one day in advance to ensure the cell growth fusion reached more than 90% the next day. Three parallel lines were drawn on the bottom of the 6-well plate in advance, the cell culture medium was aspirated, and the lines were drawn evenly with a 200 μl pipette tip perpendicular to the parallel lines to make each scratch as uniform as possible. Cells were washed with PBS to ensure no cells were floating, photographed at the intersection of the lines (localization points), recorded as 0h, and incubated with 2 ml of serum-free medium for 24h or 48h. After 24h or 48h, the medium was aspirated, washed 3 times with PBS to ensure that no cells were floating, and photographed under the microscope (at each localization point to ensure that the same area was photographed each time). ImageJ software was used to calculate the scratch area. GraphPad Prism 8.0 software was used to analyze the differences.

Preparation of CM and Jurkat cell culture experiment

RCC cells were inoculated with 5×10^6 in 10 cm cell culture dish, and the medium was changed after 24 h. The cells were incubated for another 48 h to collect conditional medium (CM). CM was centrifuged at 3000 rpm/min for 15 min to obtain the supernatant. The CM was then mixed 1:1he with complete medium for Jurkat cells culture, and the medium was changed daily. Jurkat cells were collected after 72 hours for flow cytometric analysis.

Immunoblotting and immunoprecipitation

Cells were first lysed with RIPA cell lysis solution (Solarbio, China) containing protease inhibitor and phosphatase inhibitor (MedChemExpress, USA), the lysate was separated by SDS-PAGE gel and transferred to PVDF membranes (Millipore, USA), then incubated with proteins successively according to the instructions of primary and secondary antibodies. Finally, exposure was performed using the C300 system (Azure Biosystems, USA) in the presence of an ECL luminescent solution (Millipore, USA). For immunoprecipitation, the starting steps were as described above but involved the use of IP lysate (Thermo Fisher Scientific, USA). A portion of the protein solution was taken to directly detect the corresponding protein expression, while the rest of the solution was added to the primary antibody and magnetic beads (Bimake, USA), respectively, according to the manufacturer's instructions. The beads were washed with wash buffer (Thermo Fisher

Scientific, USA) and heated to 100°C for 5 min using protein loading buffer (Abclonal, China). Immunoblotting was then performed as described above.

Establishment of mouse tumor models

Renca-WT and Renca-TOPK KD cells (1×10^6) were inoculated subcutaneously in the back of 6-8-week-old wild-type BALB/c mice. For the treatment group, Renca cell lines were inoculated with 1×10^6 cells subcutaneously on the back of 6-8-week-old wild-type BALB/c mice, and when the tumor volume grew to 50-100 mm^3, the mice were randomly divided into four groups: control group, OTS964(TOPK inhibitors) treatment group, anti-PDL1 treatment group, and combination treatment group, respectively. InVivoMAb anti-mouse PD-L1 (Bio X Cell, West Lebanon, NH, USA) or IgG isotype control (Bio X Cell, West Lebanon, NH, USA) was administered to mice at a dose of 200ug/each by intraperitoneal injection every three days. For TOPK inhibitors, the tumors were administered orally at 40 mg/kg daily, while control mice received PBS orally. Tumor volumes were measured every three days along the long axis (a) and short axis (b), and tumor volumes were calculated using the following formula: $V=ab^2/2$. Mice were sacrificed at the end of the experiment, tumors were excised and weighed, and tumor tissues were subsequently used for flow analysis, WB analysis, and immunohistochemistry, respectively.

Mouse tumor CTL isolation and flow cytometry experiments

Tumor tissues were cut and placed in DMEM solution containing 1 mg/ml collagenase IV (Solarbio, China) and in a 37°C water bath for 1 h. After digestion, the cells were placed on ice, filtered through a 100 mesh sieve(150μm), centrifuged, resuspended with 40% Percoll (Solarbio, China) and placed on the surface of 80% Percoll (Solarbio, China), and immune cells were obtained by density gradient centrifugation. The above immune cells, human kidney cancer cell lines and Jurkat cells were washed using PBS buffer and treated under dark conditions with antibodies for flow cytometry. All samples were analyzed using a Beckman Coulter CytoFLEX S flow cytometer, and FlowJo software was used to analyze the data.

Immunohistochemistry

The mouse tumor tissues were fixed in formalin, embedded in paraffin, sectioned, dried, and dewaxed in xylene, anhydrous ethanol, 95% ethanol, and 85% ethanol, respectively, then antigen repair was performed in boiled sodium citrate antigen repair solution (Thermo Fisher Scientific, USA) for 20 min, using immunohistochemical detection kit (Fuzhou Maishin Biotechnology, China). Antibody incubation was performed according to the manufacturer's instructions and observed under a microscope after hematoxylin re-staining, dehydration and sealing. Tissue Microarrays from 90 RCC patients (HKidE180Su03) were purchased from Shanghai Outdo Biotech Co.,Ltd. (Shanghai, China), and with the same process above.

QUANTIFICATION AND STATISTICAL ANALYSIS

Statistical analysis

Statistical analysis of data was performed using GraphPad Prism 8 software (GraphPad Software Inc., San Diego, CA, USA). All experiments were performed with at least three replicates, and data were expressed as mean ± standard deviation. The significance of differences between the two groups was assessed using the Student t-test. The significance of differences between multiple groups was compared using one-way and repeated measures analysis of variance (ANOVA). Correlations between variables were analyzed using Spearman's rank correlation. A p-value<0.05 was statistically significant, * for $p<0.05$, ** for $p<0.01$, and *** for $p<0.001$.